Investigation on Corrosion Behavior and Semiconductor Properties of Oxide Films on SS316L, Inconel600 and Incoloy800 in High Temperature Water with ZnO Addition

Yu TAN[*]*, Sheng-han ZHANG, Ke-xin LIANG*

School of Environment Science and Engineering, North China Electric Power University, China
[*]E-mail: lucifertan@163.com

Oxide films on 316L stainless steel, Inconel600 and Incoloy800 were formed in 288°C high temperature water with/without 650ppb ZnO addition. Corrosion resistance and semiconductor properties of oxide films on alloys after oxidation were characterized by electrochemical potentiodynamic polarization and capacitance measurement (Mott-Schottky plot).After oxidation, the surfaces of alloys with ZnO addition indicated smaller crystals than the ones without ZnO additions, supported by FE-SEM images. XPS suggested an enrichment of Zn with iron and oxygen, under the surface of oxide film on the alloys. Flat band potential of the oxide films moves to the negative direction, besides a decreasing of donor density with ZnO addition. Point defect model was employed to investigate the effect of ZnO addition on semiconductor properties of oxide films led to enhanced corrosion resistance.

1. INTRODUCTION

316L stainless steel (SS316L), Inconel600 and Incoloy800 are widely used as important component materials in nuclear power plants for their excellent corrosion resistances in high temperature water environment. Oxide films with duplex structure[1-6] forms on SS316L or Inconel600 during its exposure in high temperature water. The Zn addition (also as Zn injection, Zn treatment) into the primary circuit of BWR(boiling water reactor) is a technique to control the buildup of radiation fields from ^{60}Co out of core piping. The presence of 5-10ppb Zn^{2+} into the high temperature water of primary circuit in BWR slows the growth of oxide films on surfaces of alloys,

thereby reducing the number of sites available for the incorporation of cobalt. Zn also competes with cobalt for the sites of metal oxide during the oxidation process[7-9]. To our knowledge, the published papers about Zn addition only focused on the stress corrosion cracking. It is not clear that the impact of Zn addition on semiconductor properties of the oxide films on alloys.

Capacitance measurement is a useful electrochemical method to investigate the semiconductor properties of the oxide films which are highly related to the corrosion resistance of alloys. In recent years, it has been used to perform measurements on passive films on iron[10-11], nickel[12-13] and stainless steels[14-15]. In this work, on the basis of capacitance measurement, we paid attention to the effect of Zn addition on semiconductor properties of the oxide films formed on alloys in high temperature water condition.

2. EXPERIMENT

2.1 Materials

Commercially available SS316L, Inconel600 and Incoloy800 (Chemical composition listed in Table 1) are employed in this work. Specimens (12mm×10mm×3mm) were mechanically polished with SiC papers up to grade 2000 and then mirror finished with 0.5μm alumina gel. The specimens were, first cleaned in distilled water and second in ethanol, and then kept in a dry box.

Table 1. Chemical composition of SS316L, Incoloy800 and Inconel600 materials.

| mass fraction (wt%) | | | | | | | | |
Alloys	C	Si	Mn	P	S	Ni	Cr	Mo	Fe
SS316L	0.009	0.65	1.91	0.034	0.002	12.14	17.41	2.060	balance
Incoloy800	0.08	0.3	0.9		0.000	30.5	19.8		47.3
Inconel600	0.063	0.26	0.33	0.008	0.001	75.87	15.33		7.72

2.2 High temperature water oxidation

The oxidation process was performed in 288±2 °C water and 7.2MPa in a 1L stainless steel autoclave for 100h. The aqueous contained 650ppb ZnO and also a non-Zn baseline test (as 0 ZnO). Before oxidation start, the aqueous was deaerated by continuous bubbling with pure nitrogen gas (99.99%) for 2h. During the oxidation, the dissolved O_2 concentration was maintained less than 10ppb.

2.3 Surface analysis

After oxidation in the high temperature water, the specimens were subjected to ex-situ analyses to characterize the states of their oxidized surfaces by field emission scanning electronic microscopy

(FE-SEM) and X-ray photoelectron spectroscopy (XPS), using Al monochromator with C 1s at 284.8eV and depth profiles analyzed by Ar^+ sputtering with a rate 0.5nm/sec according to SiO_2.

2.4 Electrochemical measurements

Due to our limited technology, the oxidated specimens were investigated in "ex-situ" environment at room temperature and pressure. The electrochemical measurements were performed using a model 2273 potentiostat (Princeton) which is controlled by PowerCorr® and PowerSine® on an IBM computer. The capacitance measurements (Mott-Schottky method) were performed within the passive range that came from the result of potentiodynamic scan (without detailed expressions in this work). The measurement was applied by step of 10mV in the negative direction superimposing sinusoidal perturbing amplitude 10mV (peak to peak) with the frequency 1000 Hz. A standard three-electrode system is employed in this work as the oxidated specimen (with an area $0.28cm^2$) investigated as the working electrode. The electrolyte solution used in the electrochemical capacitance measurements was $0.15mol·L^{-1}$ boric acid and $0.0375mol·L^{-1}$ sodium borate buffered solution (pH=8.4).

3. RESULTS AND DISCUSSION

*3.1 Morphology and composition of the oxide film with Zn addition*
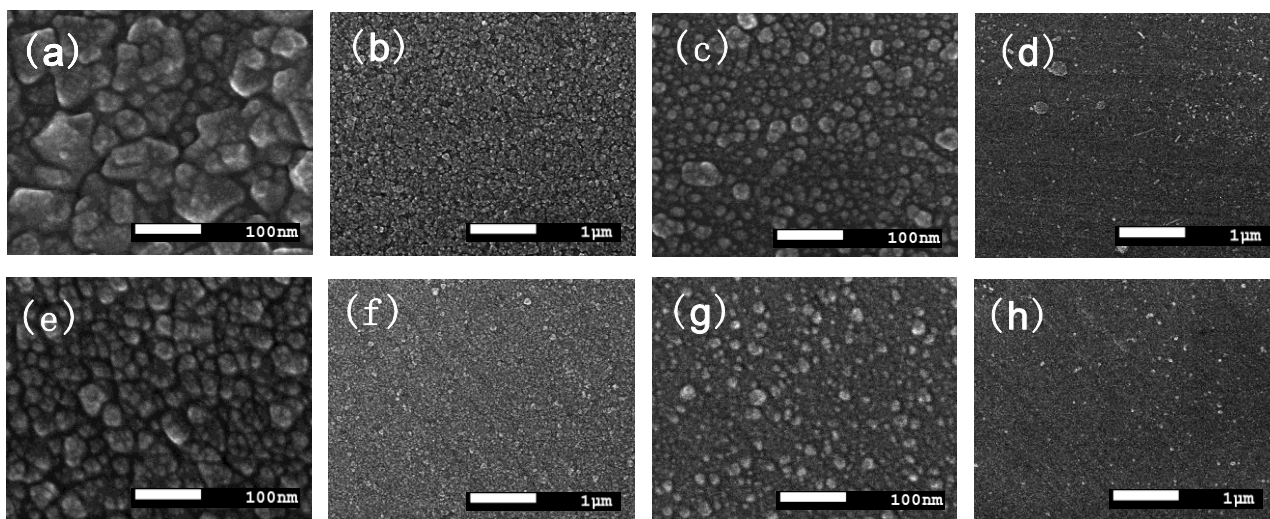
Figure 1. Morphology of the oxide films formed on 316L in high temperature water (a,b)without and (e,f)with ZnO addition, Inconel600 (c,d)without and (g,h)with ZnO addition

Visual appearances of all specimens upon removal from the autoclave remained shiny and remarkable unchanged by exposure in high temperature water with 0/650ppb ZnO addition. Figure 1 presents FE-SEM images of the oxide films of SS316L and Inconel600 after oxidation. The surfaces of

the SS316L oxidated in high temperature water condition without ZnO addition (Figure 1 a and b) were covered by two kinds of particles, sparsely larger ones and densely smaller ones. The surfaces of the SS316L oxidated with 605ppb ZnO addition (Figure 1 e and f) were densely covered by many fine particles. The size of the particles was reduced obviously and the scratches by polishing before high temperature oxidation still can be seen on the ZnO addition films. The similar results can be displayed on the surfaces of the Inconel600 oxidated in high temperature water without (Figure 1 c and d) and with ZnO addition (Figure 1 g and h). This suggested that the features of the oxide films scarcely changed after relative long-term exposure to the ZnO-free solution or ZnO-addition solution.

The depth profiles intensity of XPS of the oxide film on SS316L oxidated in high temperature water with 650ppb ZnO addition are presented in Figure 2. Besides Fe, Cr, and Ni are detected in the oxide films, Zn is also discovered. The inset shows XPS spectra of Zn in the oxide film on SS316L, an enrichment of Zn under the surface of the oxide film on SS316L where the oxygen and iron were also enriched.
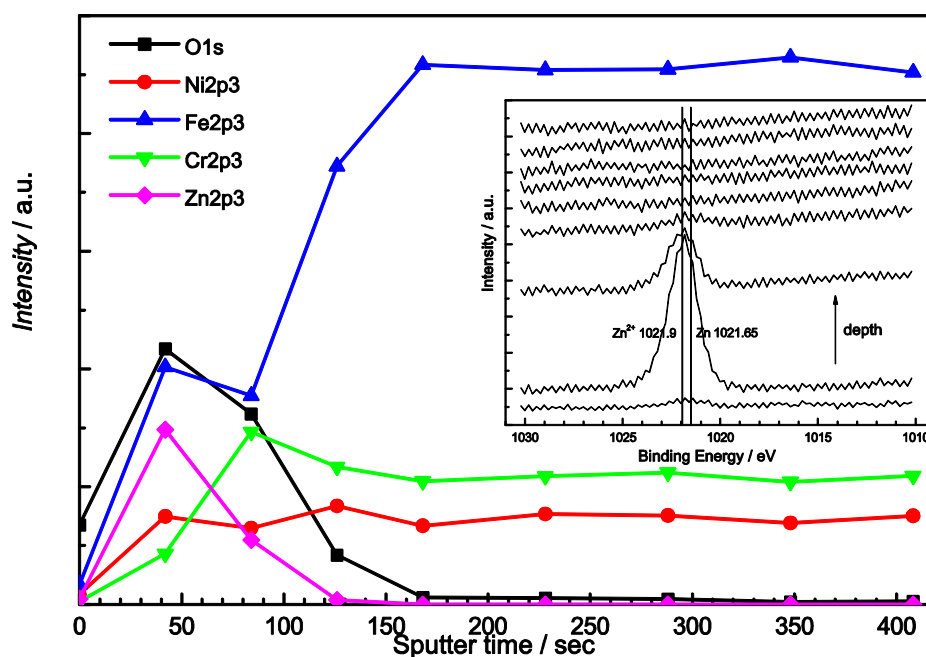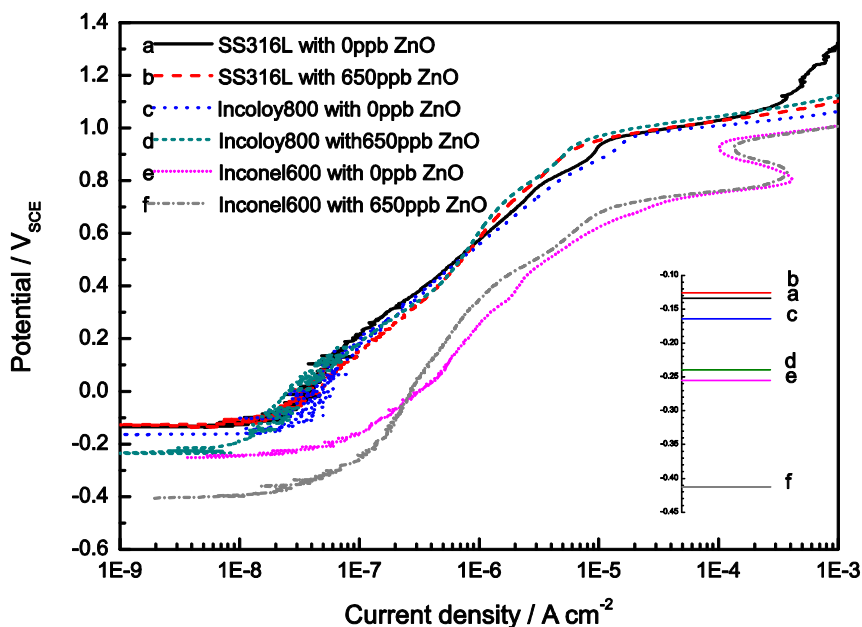

Figure 2. XPS depth profiles of the SS316L oxidated in high temperature water with 650ppb ZnO addition

3.2 Potentiodynamic polarization

The anodic potentiodynamic polarization of the specimens oxidated in high temperature water with 0/650ppb ZnO addition are plotted as Figure 3. At first the current density increases rapidly with applied potential, then increases gently as the applied potential moves to the positive direction. The current density increases dramatically when the potential is higher than the transpassive potential of about $0.95V_{SCE}$. For high composition alloys (Inconel600), there is a peak of Ni^{3+} to Ni^{6+} in the plots of Inconel600 specimen oxidated in 0/650ppb ZnO addition high temperature water. The anodic

polarization plots of the specimens shows lower average current densities of SS316L and the Incoloy800 with 650ppb ZnO addition comparing to the non-zinc ones in the range of 0.5V to the transpassive potential and the range of Inconel600 was 0V to 0.8V, respectively. The differences average current density of alloys observed on the potentiodynamic polarization plots suggested that the composition and structure of the oxide films on alloys were different with/without ZnO addition.

3.3 Capacitance measurements

Figure 3. Anodic potentiodynamic polarization plots of SS316L, Incoloy800 and Inconel600 after high temperature water oxidation with 0/650ppb ZnO addition, with scan rate of 1mV/s

The capacitance measurement by Mott-Schottky method provides precise information on the semiconductor type, density of donor or acceptor (N_D or N_A) and flat band potential (E_{fb}) of the oxide film. Figure 4 shows the Mott-Schottky plots of the oxide film on SS316L, Incoloy800 and Inconel600 oxidated in high temperature water with 0/650ppb ZnO addition. According to the published results[17-19], the oxide film on Fe and Cr indicated different semiconductor properties. In this research, The Mott-Schottky plots exhibited linear regions with positive slope, demonstrating n-type semiconductor properties, in a certain range as linear fitting in Figure 4. And discussion mainly focused on this n-type section which semiconductor properties related to the outer layer of the oxide films on alloys[4-5, 11-12]. For an n-type semiconductor, E_{fb} and N_D are estimated using the well-known equation:

$$\frac{1}{C^2} = \frac{2}{\varepsilon\varepsilon_0 e N_D}\left(E - E_{fb} + \frac{KT}{e}\right) \qquad (1)$$

Where ε is the dielectric constant of the oxide film (15.6), ε_0 is the permittivity of free space (8.854×10^{-12}F/m), e is the electron charge (1.602×10^{-19}C), K is the Boltzmann constant (1.38×10^{-23}J/K) and T is the absolute temperature. The E_{fb} was calculated from Mott-Schottky plots.

As listed in Table 2, E_{fb} of all the oxide films with 650ppb ZnO injection indicated a negative movement, besides N_D decreasing which is more significantly in the oxide films of SS316L and Incoloy800. There is a relationship between the corrosion sensitivity of alloys and the semiconductor properties of the oxide film on it.
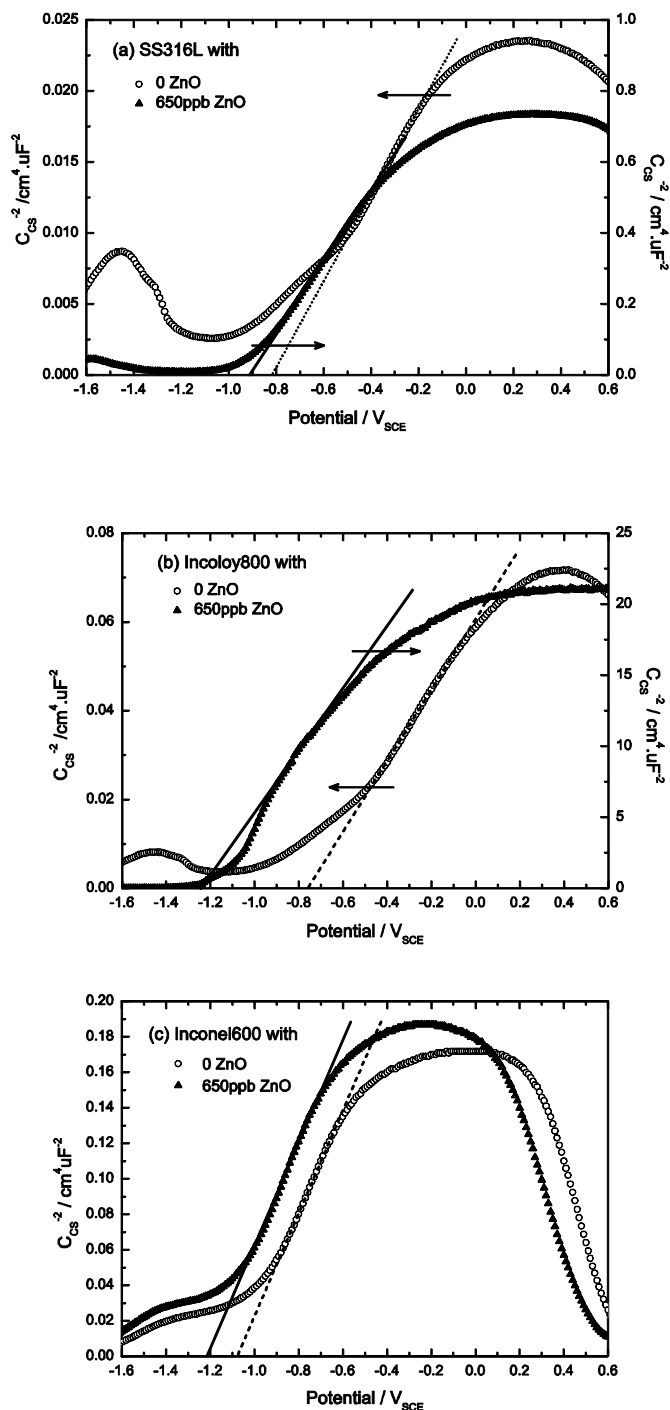
Figure 4. Mott-Schottky plots of oxide films on (a)SS316L, (b)Incoloy800 and (c)Inconel600 oxidated in high temperature water with ○0 and ●650ppb ZnO addition

According to the point defect model[20], the point defect including metal defect and oxygen vacancy in the oxide film can absorb an electro-negative ion when put into aqueous electrolyte. This absorbing evolves a new pair of hole-ion as Mott-Schottky Pair, and the metal/oxygen in this pair can evolve more related electronegative ions. That indicates the metal ions generate as an autocatalytic process which produces enrichment of metal ions on the interface of the electrolyte and the oxide film. This enrichment, when reaches a certain number, leads to the initiation of pitting corrosion or even stress corrosion cracking of the alloy. Due to the discussed above, the oxide films can be corroded easier by a higher density of acceptor/donor of the oxide film. And also in the water condition of BWRs, the oxide films with high density of acceptor/donor could be polluted easily by ^{60}Co. In this experiment, the donor density of the oxide films on alloys decreased by ZnO addition into high temperature water which indicated an enhanced corrosion resistance which is in agreement with the application in nuclear power plant[7, 9]. The high concentration of Fe in SS316L and Incoloy800 formed much iron oxide on the surfaces when corroded in the high temperature water. These iron oxides were easily impacted by ZnO addition which indicated much more changes in donor density and flat band potential of the oxide films. The depth profiles also suggested the same enrichment layer of iron and zinc in the oxide film of SS316L.

Table 2. the E_{fb} and N_D of oxide films on stainless steel and Ni-base alloys in high temperature water with 0/650ppb ZnO addition

		SS316L	Incoloy800	Inconel600
E_{fb} (mV)	0ppb ZnO	-780	-780	-1170
	650ppb ZnO	-820	-1220	-1230
$N_D(cm^{-3} *10^{18})$	0ppb ZnO	271	120	31
	650ppb ZnO	9	0.49	28

3.4 Mechanism of ZnO addition

Zinc is incorporated into the oxide films of alloys in simulated BWR condition changing the morphology and composition of oxide film, thereby changing the semiconductor properties. The reason due to the lowest (most stable) 'Site Preference Energy of metal ions in spinel lattices' of Zn^{2+}(-31.6kcal/mol) rather than Fe^{3+}(-13.3), Co^{2+}(-10.5), Fe^{2+}(-9.9), Ni^{2+}(9.0), Cr^{3+}(16.6)[9]. It suggested that Zinc displaces nickel from the crystalline lattice sites in the outer layer of oxide films on alloys. This process makes the semiconductor properties of oxide films on alloys different and the oxide films more stable and protective. The Zinc water chemistry control works well to the newly operating plant with fresh metal surface, and its corrosion inhibition effect could be displayed after a long-term Zinc injection to the plants with well-developed oxide films.

4. CONCLUSIONS

We reported an oxide films on stainless steel and Ni-base alloys formed in high temperature water with ZnO addition. The Mott-Schottky analysis indicate n-type semiconductors of oxide films on the investigated alloys after oxidation with/without ZnO addition, the flat band potential E_{fb} moves negative potential direction and the donor density N_D of the oxide films on alloys decreases for ZnO addition to the 0 Zinc ones. The spinel crystal size decreased and the number density of the crystal increased of the oxide films on alloys oxidated in the high temperature water with ZnO addition to the 0 Zinc ones.

References

1. W. F. Bogaerts, A. A. Van Haute and M. J. Brabers, *J. Nucl. Mater.*, 115 (1983) 339
2. T. L. Sudensh, L. Wijesinghe and Daniel John Blackwood, *Corros. Sci.,* 50 (2008) 23
3. Jan Macák, Petr Sajdl, Pavel Kučera, Radek Novotný and Jan Vošta, *Electrochim. Acta,* 51 (2006) 3566
4. A. Machet, A. Galtayries, S. Zanna, L. Klein, V. Maurice, P. Jolivet, M. Foucault, P. Combrade, P. Scott and P. Marcus, *Electrochim. Acta,* 49 (2004)3957
5. F. Carette, M.C. Lafont, L. Legras, L. Guinard and B. Pieraggi, *Mater. High Temp.,* 20 (2003)581
6. S.E. Ziemniak and M. Hanson, *Corros. Sci.,* 48 (2006) 498
7. Marble W.J, Diaz, Levin H.A and Garcia S.E, EPRI TR-104606, December. Palo Alto, USA; EPRI, 1994.
8. Wood Chris, *Nuclear Engineering International,* 36 (1991) 39
9. K. Fruzzetti, EPRI TR-113420, Palo Alto, USA, EPRI, 2006.
10. Scott P. Harrington, Feng Wang and Thomas M. Devine, *Electrochim. Acta,* 55 (2010) 4092
11. Shinji Fujimoto and Hiroaki Tsuchiya, *Corros. Sci.,* 49 (2007) 195
12. L.A.S. Ries, M. Da Cunha Belo, M.G.S. Ferreira and I.L. Muller, *Corros. Sci.,* 50 (2008) 676
13. Elzbieta Sikora and Digby D. Macdonald, *Electrochim. Acta,* 48 (2002) 69
14. M.J. Carmezim, A.M. Simões, M.F. Montemor and M. Da Cunha Belo, *Corros. Sci.,* 47 (2005) 581
15. M.F. Montemor, A.m.p. Simões, M.G.S. Ferreira and M. Da Cunha Belo, *Corros. Sci.,* 41 (1999) 17
16. M. Sennour, L. Marchetti, S. Perrin, R. Molins, M. Pijolat and O. Raquet, *Mater. Sci. Forum,* 595-598 (2008) 539
17. Weishan Li and Jingli Luo, *Electrochem. Commun.*, 1 (1999) 349
18. Agatino Di Paola, Deepak Shukla and Ulrich Stimming, *Electrochim. Acta,* 36 (1991) 345
19. Carmelo Sunseri, Salvatore Piazza and Francesco Di Quarto, *J. Electrochem. Soc.,* 137 (1990) 2411
20. Digby D. Macdonald, *J. Electrochem. Soc.*, 139 (1992) 3434